Mon. Not. R. Astron. Soc. **362,** 1134–1142 (2005) doi:10.1111/j.1365-2966.2005.09359.x

Hubble Space Telescope spectroscopy of the Balmer lines in Sirius B⋆

M. A. Barstow,[1]† Howard E. Bond,[2] J. B. Holberg,[3] M. R. Burleigh,[1] I. Hubeny[4] and D. Koester[5]

[1]*Department of Physics and Astronomy, University of Leicester, University Road, Leicester LE1 7RH*
[2]*Space Telescope Science Institute, 3700 San Martin Dr., Baltimore, MD 21218, USA*
[3]*Lunar and Planetary Laboratory, University of Arizona, Tucson, AZ 85721, USA*
[4]*Steward Observatory, University of Arizona, Tucson, AZ 85721, USA*
[5]*Institut für Theoretische Physik und Astrophysik, Universität Kiel, 24098 Kiel, Germany*

Accepted 2005 June 21. Received 2005 May 25; in original form 2005 April 26

ABSTRACT

Sirius B is the nearest and brightest of all white dwarfs, but it is very difficult to observe at visible wavelengths due to the overwhelming scattered light contribution from Sirius A. However, from space we can take advantage of the superb spatial resolution of the *Hubble Space Telescope* (*HST*) to resolve the A and B components. Since the closest approach in 1993, the separation between the two stars has become increasingly favourable and we have recently been able to obtain a spectrum of the complete Balmer line series for Sirius B using the *HST* Space Telescope Imaging Spectrograph (STIS). The quality of the STIS spectra greatly exceeds that of previous ground-based spectra, and can be used to provide an important determination of the stellar temperature ($T_{\rm eff} = 25\,193$ K) and gravity ($\log g = 8.556$). In addition, we have obtained a new, more accurate, gravitational redshift of 80.42 ± 4.83 km s^{-1} for Sirius B. Combining these results with the photometric data and the *Hipparcos* parallax, we obtain new determinations of the stellar mass for comparison with the theoretical mass–radius relation. However, there are some disparities between the results obtained independently from $\log g$ and the gravitational redshift which may arise from flux losses in the narrow 50×0.2 arcsec^2 slit. Combining our measurements of $T_{\rm eff}$ and $\log g$ with the Wood evolutionary mass–radius relation, we obtain a best estimate for the white dwarf mass of 0.978 $M_\odot$. Within the overall uncertainties, this is in agreement with a mass of 1.02 $M_\odot$ obtained by matching our new gravitational redshift to the theoretical mass–radius relation.

Key words: stars: abundances – stars: individual: Sirius B – white dwarfs – ultraviolet: stars.

1 INTRODUCTION

As the nearest and visually brightest example, Sirius B is one of the most important of all the white dwarf stars. Detected by Bessel (1844) through membership of a binary system, with its companion Sirius A, it provides an opportunity for an astrometric mass determination. This can be compared with other independent methods of determining stellar mass from spectroscopic temperature and gravity measurements and an observation of the gravitation redshift. Unfortunately, the proximity of Sirius B to the primary star makes most accurate spectroscopic and photometric observations extremely difficult. For example, at visible wavelengths Sirius A is approximately 10 mag brighter than Sirius B. Only at the shortest far-ultraviolet wavelengths or in the extreme ultraviolet/soft X-ray band does Sirius B become brighter than Sirius A. Of course, observations in these wavelength ranges only became possible in the space-age.

Therefore, for most of the time since its discovery astronomers have needed to make the most challenging of observations to learn about Sirius B. During this time, few useful spectra of the star were obtained. The first, by Adams (1915), revealed the enigma of white dwarf stars, showing Sirius B and Sirius A to be 'identical in all respects so far as can be judged from a close comparison of the spectra', the much lower luminosity of Sirius B placing it in the lower-left corner of the Hertzsprung–Russell (HR) diagram along with 40 Eri B. From subsequent observations, Adams (1925) reported a first gravitational redshift. However, along with that reported by Moore (1928), the value was a factor of 4 too low due to contamination of the spectra by Sirius A (see discussions by Greenstein, Oke & Shipman 1971, 1985; Wesemael 1985). For example, the results depended on measurements of metallic lines such as Mg II 4481 Å, which are now known not to occur in most white dwarfs. Indeed,

⋆Based on observations with the NASA/ESA *Hubble Space Telescope*, obtained at the Space Telescope Science Institute, which is operated by AURA, Inc., under NASA contract NAS5-26555.

†E-mail: mab@star.le.ac.uk

a reliable redshift (89 ± 16 km s^{-1}) was only eventually published by Greenstein et al. (1971) based on a photographic plate obtained in ∼1963.

Greenstein et al. (1971) also published measurements of the effective temperature and surface gravity of Sirius B, based on their analysis of the Hα and Hγ profiles, of $32\,000 \pm 1000$ K and $\log g = 8.65$, respectively. However, measurements based on only a few such line profiles can be prone to ambiguities in the determination of these parameters. Also, modern computational fitting techniques allow a complete objective exploration of the available parameter space compared to the visual comparisons available to Greenstein et al. (1971). While the effective temperatures of DA white dwarfs can be formally measured to an accuracy of ∼1 per cent between 20 000 and 30 000 K, with access to the complete Balmer line series from Hβ to H8 (see Finley, Koester & Basri 1997; Liebert, Bergeron & Holberg 2005), estimates of $T_{\rm eff}$ for Sirius B have ranged from the Greenstein et al. value down to as low as 22 500 K (Koester 1979). The availability of low dispersion *International Ultraviolet Explorer* (*IUE*) and *EXOSAT* spectra refined the value of $T_{\rm eff}$ to $26\,000 \pm 2000$ K (Holberg, Wesemael & Hubeny 1984; Paerels et al. 1988; Kidder, Holberg & Wesemael 1989). Most recently, Holberg et al. (1998) have combined the *IUE* NEWSIPS data and the *Extreme Ultraviolet Explorer* (*EUVE*) spectrum to produce a new, well-defined effective temperature of $24\,790 \pm 100$ K and surface gravity of $\log g = 8.57 \pm 0.06$. Coupled with the *Hipparcos* parallax of $\pi = 0.37921 \pm 0.00158$ arcsec and the Greenstein et al. gravitational redshift, Holberg et al. obtained a white dwarf mass of 0.984 ± 0.074 M$_\odot$ and a radius $R = 0.0084 \pm 0.00025$ R$_\odot$. This spectroscopic result is consistent with the astrometric mass of Gatewood & Gatewood (1978) and the joint spectrometric and astrometric constraints are within 1σ of the most recent thermally evolved mass–radius (M–R) relations of Wood (1992, 1995). Some of these earlier measurements are summarized in Table 2. Nevertheless, the spectroscopic uncertainties remain large at 7.5 per cent in mass and 4 per cent in radius. A precise test of the mass–radius relation for a ∼1-M$_\odot$ white dwarf that can distinguish between different evolutionary models, for example, between thick and thin H layer, masses, requires significantly reduced errors on the measured spectroscopic parameters. While important improvements were achieved by Holberg et al. (1998), it is clear that the Balmer line technique provides results of potentially greater accuracy if such a spectrum could be obtained free from contamination by Sirius A.

The paper of Greenstein et al. (1971) does not reproduce the original photographic plate images, plotting just the scanned Hα and Hγ profiles. Hence, it is difficult to judge the level of contamination from Sirius A in their work. Nor in any of the earlier works are the original photographic plates reproduced in the literature. Therefore, a photographic spectrum obtained and published by Kodaira (1967) is of particular importance. This plate covers the Balmer line series from Hγ through to H10 and the spectrum of Sirius B is clearly visible in the middle of scattered light contributions from the diffraction spikes of Sirius A. It also illustrates the particular difficulty of observing the Sirius B from the ground because, even with ∼1-arcsec 'seeing', the spectrum sits on a scattered light component ∼1/4 to 1/3 of its total flux.

Clearly, a visible band observation of Sirius B would be much better carried out in space, reducing considerably the problems discussed above. The *Hubble Space Telescope* (*HST*) was the first instrument capable of obtaining such a spectrum, but for some time following its launch Sirius B has been in an unfavourable position relative to Sirius A, making its closest approach (as projected on the plane of the sky) during 1993. However, as the distance between the two binary companions has increased and we have obtained high-quality direct images of the system with the *HST*, it has become feasible to obtain a Balmer line spectrum of Sirius B. We report here on the analysis of the spectrum acquired with the Space Telescope Imaging Spectrograph (STIS) during 2004, obtaining measurements of $T_{\rm eff}$ and $\log g$, a new gravitational redshift and a revised estimate of the visual magnitude, from which we determine the white dwarf mass and radius.

Table 1. Details of the STIS observations of Sirius B.

Grating	λλ range	Resolution (Å)	File ID	Exposure time (s)
G430L	2900–5700	5.5	O8P901010	10.5
G750M	6265–6835	1.1	O8P901020	90.0

2 STIS OBSERVATION OF SIRIUS B

Sirius B was observed with STIS on 2004 February 6, using the G430L and G750M gratings, to obtain coverage of the full Balmer line series (see Table 1). Even though the *HST* has the advantage of operating above the atmosphere, acquisition of a spectrum uncontaminated by Sirius A remains a challenge, particularly as the length of the spectrograph slit (52 arcsec) is considerably greater than the dimensions of the Sirius system. As the orbit of Sirius is well determined, it is quite straightforward to avoid placing Sirius A on the slit at the same time as Sirius B. However, it is inevitable in avoiding the primary that its diffraction spikes must then cross the slit and may potentially contaminate the Sirius B spectrum. To reduce the level of contamination in the Sirius B spectrum to the lowest possible level, we chose a spacecraft orientation such that the target was equidistant between the locations of the Sirius A diffraction spikes. Although we devised this approach independently, it is interesting to note that this same technique was adopted by Kodaira (1967), although with less freedom available in the slit orientation. This is illustrated in Fig. 1, which shows our most recent *HST* Wide Field Planetary Camera 2 (WFPC2) image of the Sirius system, obtained as part of an ongoing programme of imaging with which we are continually improving the astrometric orbit

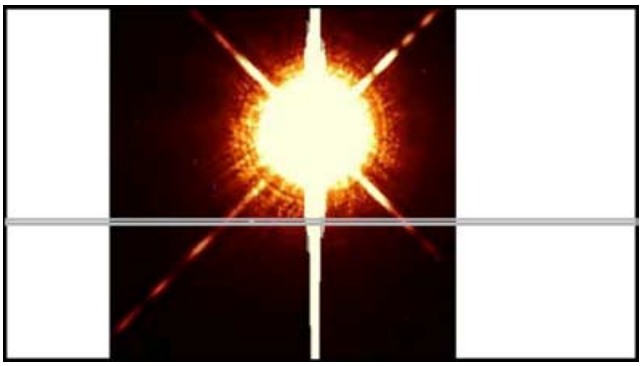

Figure 1. *HST* WFPC2 image of the Sirius system showing the overexposed image of Sirius A, with its four diffraction spikes. The vertical bar is the 'bleed' of Sirius A into adjacent pixels along the readout columns of the CCD, due to the overexposure. Sirius B lies just to the right of the bottom-left diffraction spike. The grey box represents the dimensions of the 52×0.2 arcsec^2 slit, which cuts across Sirius B and two of the diffraction spikes.

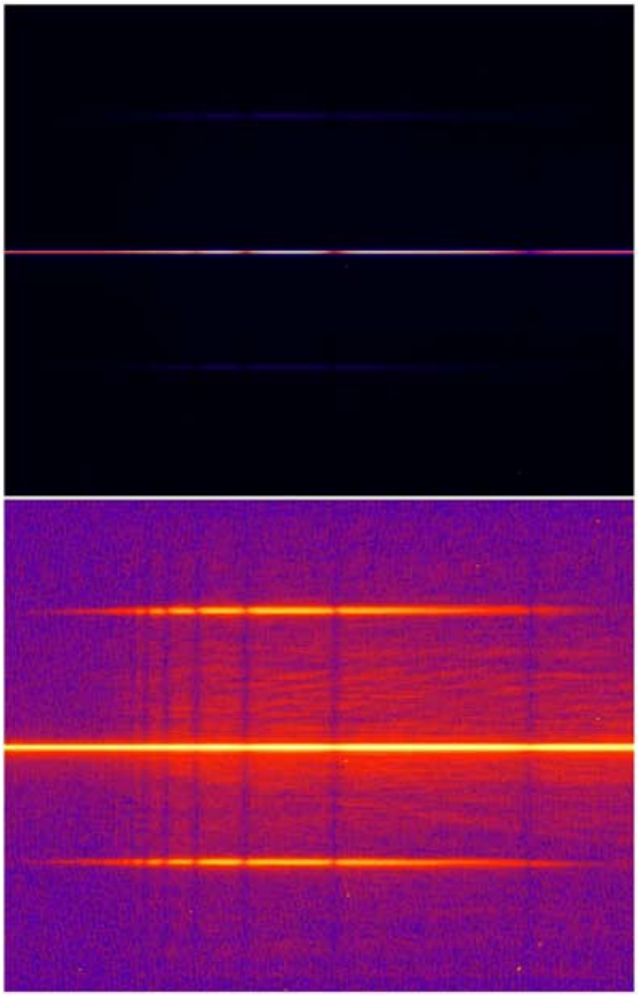

Figure 2. Top: image of the G430L spectrum of Sirius B (centre), with the spectra of the diffraction spikes of Sirius A (top and bottom) on a linear intensity scale. Bottom: the same image plotted on a logarithmic scale to enhance the background and scattered light components.

determination and, ultimately, the Sirius B astrometric mass. The image shows the overexposed image of Sirius A, with its four diffraction spikes. The vertical bar is the 'bleed' of Sirius A into adjacent pixels along the readout columns of the CCD, due to the overexposure. Sirius B lies just to the right of the bottom-left diffraction spike. The grey box represents the dimensions of the 52×0.2 arcsec^2 slit, which cuts across Sirius B and two of the diffraction spikes. Note that in the spectroscopic exposure, the main Sirius A image is obscured and the vertical overexposed columns would not be present. With relative freedom to choose the roll angle of the *HST* during the spectroscopic exposures, we selected an orientation that placed Sirius B almost exactly halfway between two of the diffraction spikes from Sirius A, in the direction perpendicular to the bleeding columns.

The G430L and G750M spectra were each obtained as a series of three separate exposures to maximize the signal-to-noise, while preventing saturation of the CCD, and for cosmic ray rejection. The CCD image of the G430L observation is shown in Fig. 2. Uppermost is the image displayed with a linear intensity scale, which shows the well-separated spectra of Sirius B (centre) and the fainter Sirius A diffraction spikes (top and bottom). Absorption dips from the

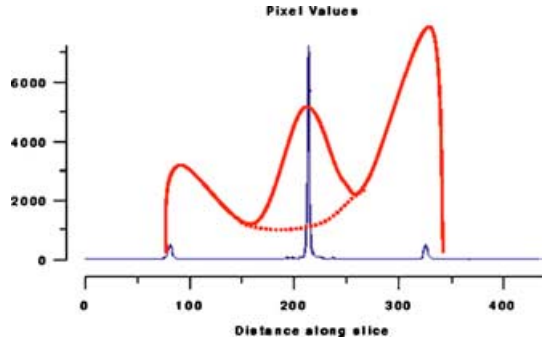

Figure 3. Vertical slice through the image in Fig. 2 showing the relative intensities of the three spectra. For comparison, we also show a slice through the spectrum of Kodaira (1967) normalized to the same intensity and spatial scale. The dotted line is an extrapolation of the diffraction spike flux to show the level of contamination in the spectrum of Sirius B.

Balmer lines can be clearly seen in all the spectra. Hβ is to the right of the image and the converging series limit to the left. Below this is the same image using a logarithmic intensity scale, which enhances the lower flux levels showing the background and scattered light components. The presence of the Balmer absorption line in the background shows it to be dominated by the scattered light from Sirius A.

To demonstrate the relatively low level of the scattered light, we display a cut through the image in Fig. 3. Also shown is an equivalent slice through the spectrum of Kodaira (1967), copied from the original paper and normalized to the same intensity and spatial scale as the *HST* data. This illustrates very clearly how the ground-based observation has been compromised by the difficulties with 'seeing'. In the *HST* image, the diffraction spikes have a much lower intensity than Sirius B and the diffraction limited imaging provides a clear separation of the spectra. Although the scattered light component can be seen in the heavily contrast enhanced lower image of Fig. 2, it is barely detectable in the intensity histogram. We estimate that the scattered light component is very much less than 1 per cent of the flux of Sirius B in the G430L observation and is $\sim$2 per cent in the G750M grating exposure.

3 ANALYSIS OF THE BALMER LINE SPECTRUM OF SIRIUS B

3.1 Spectroscopy

The G430L and G750M spectra of Sirius B were each obtained as a series of three exposures to achieve the best possible signal-to-noise while avoiding saturation of the CCD and to facilitate removal of cosmic rays. These were automatically combined in the standard STIS CCD pipeline before the Sirius B spectrum was extracted, background-subtracted and calibrated (see Kim Quijano et al. 2003). Both resulting spectra are shown in Fig. 4. It can be seen that the Hα line profile (right) shows a slight 'roll-off' in the flux towards short wavelengths. Any light loss from the slit should be wavelength-independent, suggesting that this is a calibration artefact. A similar feature is seen in the G750M spectrum of G191−B2B (Proffitt, private communication). Therefore, we did not include the Hα profile in the determination of temperature and gravity.

Our standard technique (along with many other authors; see, for example, Bergeron, Saffer & Liebert 1992; Barstow et al. 2003a) has been to simultaneously compare the Hβ–Hε lines with synthetic

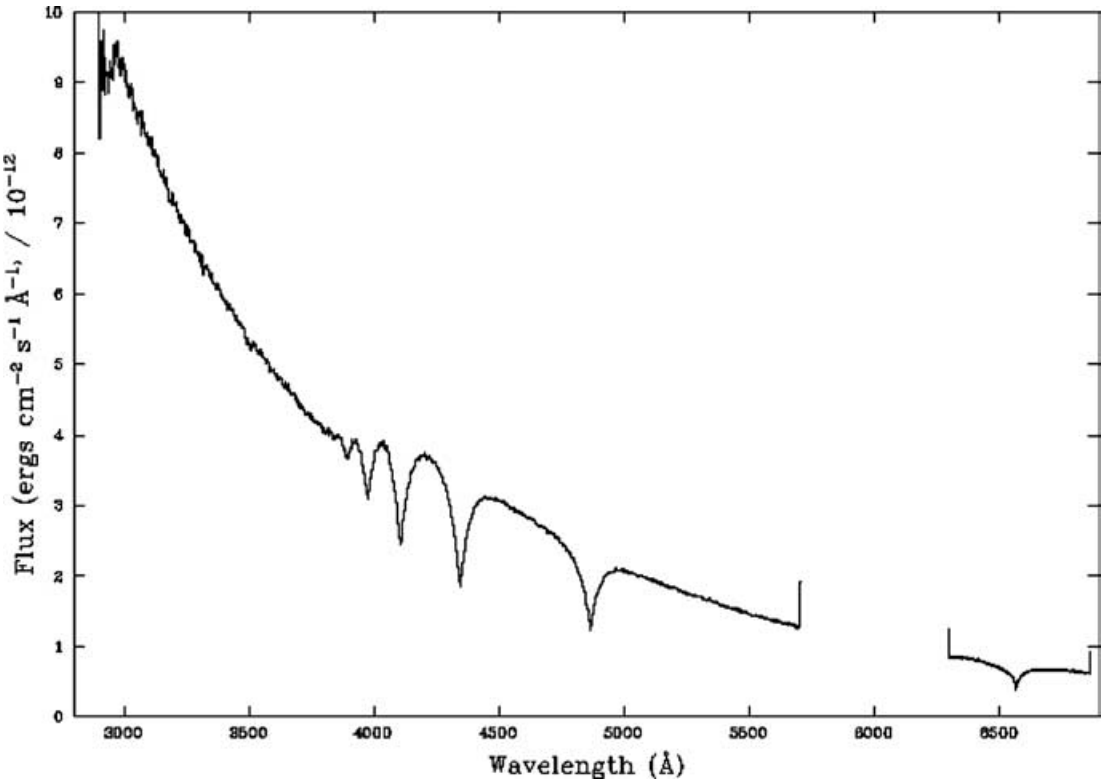

Figure 4. Flux calibrated and background subtracted spectra of Sirius B obtained, as described in the text, with the G430L (3000–5700 Å) and G750M (6300–6900 Å) gratings of the STIS instrument on the *HST*.

stellar spectra and use a χ^2 fitting technique to determine the best value of $T_{\rm eff}$ and $\log g$. These models have been thoroughly described elsewhere (e.g. Barstow et al. 2003a,b). To take account of the possible systematic errors inherent in the flux calibration of ground-based spectra, we have usually applied an independent normalization constant to each line. However, in the case of the *HST*, there is no atmospheric attenuation to deal with, removing one of the primary uncertainties in the flux calibration process. Furthermore, partly as a result of this, the calibration of the STIS instrument is extremely accurate and stable. The absolute flux scale is based on four primary DA white dwarf standards (G191−B2B, GD153, GD71 and HZ43), which are pure hydrogen models normalized to Landolt V-band photometry, which yields absolute fluxes determined to ∼4 per cent in the far-ultraviolet and to ∼2 per cent at longer wavelengths (Bohlin 2000; Bohlin, Dickinson & Calzetti 2001). Photometric repeatability is in the 0.2–0.4 per cent range. With such accuracy and repeatability, we have fit the complete spectrum of Sirius B covering the Balmer lines from Hβ down to the series limit, a wavelength range from ∼5200 to 3800 Å. We used a χ^2 statistic to determine the values of $T_{\rm eff}$ and $\log g$ that yield the best agreement between the model and data. The result of this analysis is shown in Fig. 5, with the best-fitting values and their associated uncertainties listed in Table 2. We note that a standard analysis of the individual lines (discussed above) yields similar results but with larger uncertainties.

The ∼0.15 per cent errors on $T_{\rm eff}$ and $\log g$ quoted in Table 2 are remarkably small and represent the formal internal errors arising from the spectral analysis. However, they only take into account the statistical errors on the data points and do not deal with any systematic errors arising from the analysis procedure, data reduction and or calibration. It is important to question how realistic these are in the light of the magnitudes estimated by other authors. For example, Bergeron et al. (1992) quote typical errors 350 K (∼1.5–2 per cent) in $T_{\rm eff}$ and 0.05 dex in $\log g$ for their sample of DA white dwarfs, while Finley et al. (1997) find internal errors of 1 per cent and 0.02 dex, respectively. Probably the best and most consistent set of Balmer line analyses is that carried out for the Palomar Green (PG) sample by Liebert et al. (2005). Their internal uncertainties are 1.2 per cent in $T_{\rm eff}$ and 0.038 dex in $\log g$. These are ground-based results. We are operating in uncharted territory as our space-based STIS spectrum is virtually unique in its high signal-to-noise and spectrophotometric fidelity. On the other hand, we do not have other observations to help assess the reliability of the quoted errors. Taking a conservative approach we would adopt errors typical of those obtained from the ground-based studies. However, in the context of the systematic uncertainties reported in the latter sections of this paper these spectral analysis errors are small and do not contribute significantly to overall error budget.

3.2 Photometry

One of the primary sources of uncertainty in the analysis of most previous Sirius B data has been the lack of accurate photometry. Traditionally, this has meant measuring or estimating the V magnitude of the white dwarf. In most past work (e.g. Holberg et al. 1998), we have used the estimate of $V = 8.44 \pm 0.06$ from Holberg et al. (1984), which in turn was based on an average of various published measurements. With the high spectrophotometric accuracy of the *HST* calibration, we have a first opportunity to determine magnitudes for Sirius B in various bands that have an equivalent accuracy

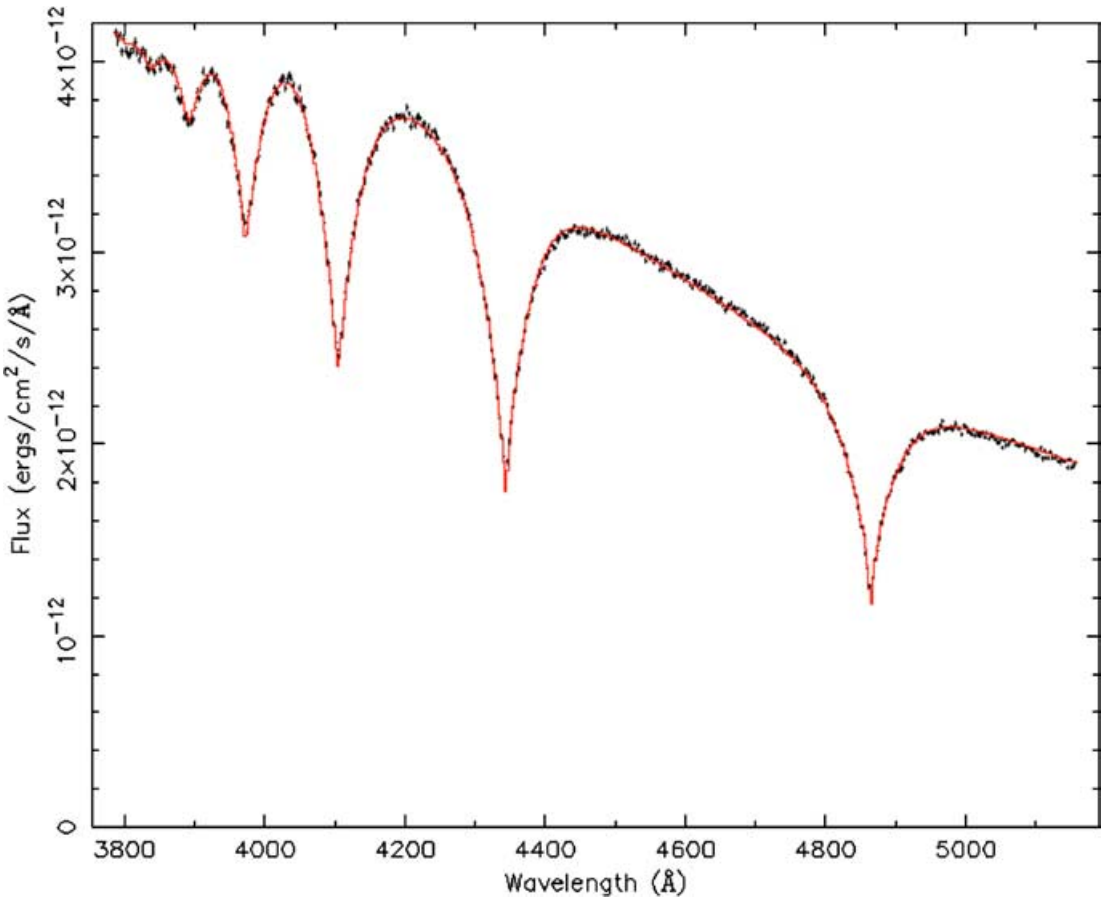

Figure 5. Section of the G430L Sirius B spectrum spanning the wavelength range 3800–5200 Å (small black crosses, size indicating the statistical errors) with the best-fitting synthetic spectrum (smooth curve – red on-line) corresponding to $T_{\rm eff} = 25\,193$ K and $\log g = 8.556$.

Table 2. Summary of the physical parameters of Sirius B measured or reported by Holberg et al. (1998), except for the redshift, which is from Greenstein et al. (1971). These values are compared with the most recent results that we have obtained from analysis of the *HST* STIS G430L and G750M spectra. The mass and radius are from the spectroscopic results only and do not take account of the astrometric values.

Parameter	Value	Error	*HST*	Results
m_V	8.44	0.06	8.528	0.05
$T_{\rm eff}$ (K)	24,790	100	25,193	37
$\log g$	8.57	0.06	8.556	0.010
π (arcsec)	0.37921	0.00158		
$V_{\rm gr}$ (km s^{-1})	89	16	80.42	4.83
M ($M_\odot$)	0.984	0.074	See Table 5	
R ($R_\odot$)	0.0084	0.00025	See Table 5	

to that easily obtained for other white dwarfs where photometric contamination is not an issue.

We can use our observed G430L spectrum to define a model atmosphere spectrum, which accurately represents the absolute Sirius B flux distribution, both in level and in spectroscopic detail. The usefulness of such a model is twofold. First, it covers wavelengths outside the range of the G430L spectrum. Secondly, it provides a noiseless numerical representation of the absolute spectrum, which can be accurately convolved with various filter functions to give synthetic magnitudes in different bands. The method that we use begins with the new absolute spectrophotometry of Vega (α Lyrae) presented in Bohlin & Gilliand (2004). These authors directly measured the absolute flux of Vega using the STIS CCD and various gratings covering the wavelength range 1700 Å to 1 μm. A new V magnitude (0.026 ± 0.008) and new absolute flux at 5556 Å (3.46×10^{-9} erg cm^{-2} s^{-1} Å^{-1}) were also determined. Bohlin & Gilliland estimate the uncertainty in the Vega fluxes to be better than 1 per cent. More importantly, Vega is now directly on the same *HST* white dwarf flux scale used to define the STIS calibration, and hence our Sirius B fluxes. We can therefore convolve any well-defined set of relative filter functions with the Vega flux distribution to derive appropriate flux zero-points for each filter. Convolution of the same filter functions with the Sirius B spectrum, together with the application of the flux zero-points, gives the synthetic magnitudes of Sirius B for each filter. Further, it is a simple matter to confirm these procedures by applying the same filter functions and zero-points to the set of four fundamental white dwarfs (GD 71, GD 153, HZ 43 and G191B2B), which define the *HST* calibration system and to verify that the resulting synthetic magnitudes match the observed ground-based magnitudes.

In seeking to minimize the effect of scattered light from Sirius A, we chose to use the small 0.2-arcsec slit for both spectroscopic observations. This is also important for obtaining the best possible spectral resolution for the gravitational redshift measurement (see Section 3.3). Therefore, although the nominal absolute calibration of the *HST* spectrographs is ∼1 per cent, we must also consider the light losses associated with this narrow slit. There are two distinct effects. First, recent adjustments to the flux calibration are

not included in the standard pipeline. These are not, as yet, documented formally but have been supplied to us by C. R. Proffitt (private communication). For the G430L grating and 52×0.2 arcsec^2 aperture, the flux measurement from the pipeline is overestimated by a smooth wavelength-dependent factor ranging from ∼5 to 7 per cent. Accordingly, we have corrected the measured fluxes used in the analyses reported here using the appropriate function. There are insufficient calibration data available for a similar analysis to be carried out for the G750M 52×0.2 arcsec^2 aperture combination.

While light losses, arising from the use of the small aperture, are in principle taken into account in the calibration pipeline, there is an enhanced scatter in the accuracy of the flux determination due to stochastic effects on the placement of the source in the slit. Bohlin (1998) estimates this to have an rms value of 4.5 per cent for the 52×0.2 arcsec^2 slit, dominating the 1 per cent absolute calibration error, which yields a 0.05-mag uncertainty in the photometry. Therefore, the uncertainty that we can assign to the synthetic magnitudes and fluxes measured here will be correspondingly greater than the formal absolute error. However, we note that the increased uncertainty associated with light loss in the slit can only be single-sided, as flux can only be lost and not gained relative to the true brightness. Therefore, any determination of the flux, and the corresponding magnitudes, has an asymmetric range of uncertainty of +5 and −1 per cent.

We have chosen the *UBVRI* filter responses defined by Cohen et al. (2003) for this work. These include detailed atmospheric transition modifications to the Landolt (1992) *UBVRI* filter functions. Bohlin & Gilliland use the Cohen et al. *V*-band filter function to establish their *V* magnitude for Vega. In addition to the Cohen et al. *UBVRI* filter functions, we also use the observed *V* magnitudes of Vega from Bessell, Castelli & Plez (1998), except for *V* where we use the Bohlin & Gilliland Vega *V* magnitude. The relation between integrated fluxes, $F_{\rm int}$, the Vega magnitudes and filter constants is given in equations (1) and (2):

$$F_{\rm int} = \frac{\int f(\lambda) S(\lambda)\, {\rm d}\lambda}{\int S(\lambda)\, {\rm d}\lambda} \quad (1)$$

$$\text{Filter const.} = \text{Vega mag.} + 2.5 \log(F_{\rm int}). \quad (2)$$

Here, $f(\lambda)$ is the Vega flux and $S(\lambda)$ is the relative filter response function. In Table 3 we provide the results of these calculations for Sirius B, the *UBVRI* filters, including the logs of the flux zero-points, the observed Vega magnitudes and synthetic Sirius magnitudes for each filter.

Using these same procedures for GD 71, GD 153, HZ 43 and G191 B2B, the absolute values of the differences between the synthetic and the observed (Landolt) magnitudes are less than 0.007 mag for each filter, except for the *U* band. The numerical definition of the *U* filter function extends shortward of the atmospheric cut-off and thus will not correspond to any observed *U* magnitude. Our synthetic Sirius B *U* magnitude therefore represents a hypothetical observation above the Earth's atmosphere rather than any realizable ground-based observation. Because our calculations are self-consistent with respect to the *HST* flux scale, we have set the uncertainties for each magnitude to 0.05 mag to accommodate the estimated uncertainty in that scale and to take account of the small, 0.2 arcsec, aperture used in the observations. This is not much smaller than the uncertainty obtained by Rakos & Havlen (1977). Using $V = 8.528 \pm 0.05$ and our adopted trigonometric parallax for Sirius B, we find an absolute magnitude of $M_v = 11.427 \pm 0.05$.

Table 3. Synthetic photometry of Sirius B.

Band	Vega Mag.	Filter Const.	Sirius B Mag.
U	0.0240	−21.0020	7.256 + 0.01/−0.05
B	0.0280	−20.4477	8.394 + 0.01/−0.05
V	0.0260	−21.0503	8.528 + 0.01/−0.05
R	0.0370	−21.6061	8.656 + 0.01/−0.05
I	0.0330	−22.3704	8.802 + 0.01/−0.05

3.3 Gravitational redshift

The primary aim of obtaining the higher-resolution G750M spectrum was to use the narrow Hα core to obtain a gravitational redshift for Sirius B. To do this, we cross-correlated a synthetic Hα profile, computed for the temperature and gravity determined for the other Balmer lines, with the observed line and calculated the relative Doppler shift between the two using a χ^2 minimization technique. With the narrow Hα core, this technique yields a formal fractional uncertainty in z of ∼1 per cent.

With such precision, it is important to consider any systematic effects that might contribute to the overall uncertainty. For example, with a predicted redshift of ∼70 km s^{-1} (before correction for γ and K velocities), the observed wavelength shift will be ∼1.5 Å. Therefore, it is necessary to use a reference wavelength for Hα that is accurate to better than 0.01 Å. Accordingly, we have recalculated the wavelength of Hα from the weighted mean of the fine structure energy levels, obtaining a value of 6564.6271 Å in vacuum, which we adopt for this analysis. We note that, although we are dealing with visible light wavelengths for which the wavelength calibration is usually carried out in air (for ground-based telescopes), the STIS calibration refers to vacuum at all wavelengths.

Although we take account of Stark broadening in calculating the profiles of the Balmer (and Lyman) lines in the synthetic spectra, using the tables of Lemke (1997), we have not routinely considered the possible Stark shifts of the lines. These are predicted to be quite small but are always in the redward direction and could contribute to an increased redshift measurement compared to the true gravitational value. Greenstein et al. (1971) estimated such a shift to be about 8 km s^{-1}, based on the data of Wiese & Kelleher (1971). In the context of the ±16 km s^{-1} uncertainty in their redshift measurement, this is not significant and the magnitude of the Stark shift was not considered further, due to the noise in the Wiese & Kelleher (1971) data for small shifts and the complexity of the radiative transfer problem. However, compared to our redshift measurements, which have a formal 1 per cent accuracy, this ∼10 per cent contribution to the measured redshift (equivalent to ∼0.15 Å in the measured wavelength shift) would be extremely important. However, the reported possible shifts are highly dependent on the plasma density, which is determined by the Balmer line formation depth. A full radiative transfer treatment is needed to determine whether or not the Stark pressure shift makes a significant contribution to the measured redshift. Consequently, we have modified the spectral synthesis program SYNSPEC to include the effect of Stark shifts in the calculation of the Balmer and Lyman line profiles. We followed the procedure outlined by Grabowski et al. (1987). For a white dwarf of the temperature and gravity of Sirius B, the additional Stark shift predicted by the new spectral synthesis calculations is tiny and does not need to be considered in this (or any) analysis.

The Hα line extends across ∼300 pixels of the G750M spectrum. It is possible to use just the narrow line core or the core and wings for the redshift measurement. It is debatable whether using the narrow

Table 4. Redshift measurements made for different pixel ranges centred on the wavelength of the Hα line.

Pixel no	z	$\Delta\lambda$	v (km s^{-1})
14	2.4083×10^{-4}	1.581	71.82
114	2.4404×10^{-4}	1.602	72.45
214	2.2500×10^{-4}	1.477	68.71
314	2.2332×10^{-4}	1.466	68.35
Mean			70.33 ± 1.82

Table 5. The mass and radius of Sirius B calculated for the different values of R related to the normalization constant determined for each of the gratings used.

Grating	G430L	G750M
R^2/D^2	4.662×10^{-21}	4.996×10^{-21}
$R_\odot$ ($\times 10^{-3}$)	$8.004 + 0.372/-0.081$	$8.330 + 0.383/-0.083$
$M_\odot$ (g)	$0.841 + 0.080/-0.026$	$0.911 + 0.084/-0.027$
$M_\odot$ (V_{gr})	1.012 ± 0.060	1.050 ± 0.063

core alone or making use of the additional information available in the line wings is the best approach. Table 4 records the observed wavelength shift and corresponding velocity for several different pixel ranges. There is a significant scatter in the values obtained, compared to the formal statistical errors, indicating the possible level of any systematic errors. In our further analysis, we adopt the mean of these redshift values and their standard deviation as an indication of the true uncertainty in the measurement. In addition, we must also consider the uncertainty in the calibration of the wavelength scale, which is ~0.2 pixel (0.12 Å) for the narrow slit, giving a total uncertainty of 6 per cent of the measured redshift.

To convert this into a gravitational redshift it is necessary to take account of the radial velocity of Sirius B, which consists of the gamma velocity of the system and the K velocity of Sirius B. The apparent velocity is the algebraic sum of the gravitational redshift, the orbital velocity of Sirius B and the γ velocity of the system barycentre. We have independently determined the latter two quantities in order to estimate the intrinsic gravitational redshift of the white dwarf (Holberg, in preparation). The system velocity or γ velocity can be directly determined from the apparent radial velocity of Sirius A as a function of time. Holberg (in preparation) has fit the published velocities of Sirius A allowing the constant γ velocity to vary as a free parameter. The observed velocities were taken from the literature and included early, turn of the last century, photographic measurements as well as more recent CCD observations from nine observatories. In most instances the data points represented annual or semi-annual averages from a given observatory. Where uncertainties were not provided, they were estimated from the standard deviations of the means or were assigned a value as typical for a given observatory at that period. No attempt was made to adjust velocity zero-points between different observatories. Several obviously discrepant observations were excluded. The direct χ^2 fit for the γ velocity yields -7.85 ± 0.72 km s^{-1}. The result is only very weakly dependent on any reasonable selection of orbital parameters and stellar mass ratio and is in good agreement with earlier results obtained by Campbell (1905), Aitken (1918) and van den Bos (1960): -7.4, -7.37 and -7.43 km s^{-1}, respectively. None of these earlier results, however, appears to have corrected for the gravitational redshift of Sirius A ($+0.75$ km s^{-1}). When this correction is applied, the resulting value of $\gamma = -8.60 \pm 0.72$ km s^{-1}. The orbital Doppler velocity of Sirius B on 2004 February 6 (-1.49 km s^{-1}) can be obtained directly from the work of Holberg (in preparation). Thus, the additive correction to be applied to our apparent Doppler velocity of Sirius B is -10.09 ± 0.72 km s^{-1}, yielding a value of 80.42 ± 4.83 for the gravitational redshift of the white dwarf.

4 DISCUSSION

We have presented an initial analysis of the first Balmer line spectrum of Sirius B obtained from space. While this is not the only Balmer line spectrum obtained, it is certainly the only one to have eliminated the problem of the scattered light from Sirius A, providing a clean background subtracted spectrum from which accurate determinations of $T_{\rm eff}$, $\log g$ and the gravitational redshift can be made. It is clear, from Tables 2 and 5, that the uncertainties in the determination of all these parameters are considerably improved from their earlier values. Within the quoted errors, the values obtained in this work are mostly compatible with the previous determinations, apart from $T_{\rm eff}$. However, it is important to note that the older measurements of $T_{\rm eff}$ and $\log g$ were made using a previous generation of stellar atmosphere calculations, which might explain the difference between the temperature values. A thorough analysis of other data sets with the most recent models will be required to resolve this.

With improved measurements of the physical parameters of Sirius B, it should now be possible to improve the accuracy of the determination of the mass and radius and, as a result, provide a more definitive test of the white dwarf mass–radius relation.

4.1 Radius and mass of Sirius B

Rather than calculating the photometric radius of Sirius B from the synthetic V magnitude, it is more straightforward to simply use the normalization applied to the best-fitting spectral model to match the observational data. This conveniently defines the stellar solid angle (R^2/D^2). Using our adopted trigonometric parallax, we can then calculate the white dwarf radius directly. We have performed this exercise for both our G430L and G750M data, as summarized in Table 5. The observational uncertainties in R are dominated by the systematic errors in the *HST* flux scale. It can be seen that the values of R^2/D^2 and R are not identical for each grating, although they do agree within the identified systematic uncertainties. We note that the G430L flux scale has had a flux scale correction applied that is not included in the pipeline processing (as discussed in Section 3.2). No similar correction could be applied to the G750M data because the relevant calibration information is not available.

Having determined the radius of Sirius B, there are two independent ways that we can estimate its mass from the available data, using relations including the surface gravity or the gravitational redshift:

$$g = GM/R^2 \qquad V_{\rm gr} = 0.636M/R. \tag{3}$$

Because there are two estimates for the stellar radius, we have made separate calculations of the mass using each of these (Table 5).

It is clear that the two different methods of estimating the white dwarf mass are giving us different answers. However, within the overall uncertainties that we have uncovered in the flux and wavelength calibration, the results are formally more or less compatible but at the very extremes of the range within which they remain consistent. Indeed, the 1σ ranges of M determined for the radius derived from the G430L flux level do not quite overlap. This

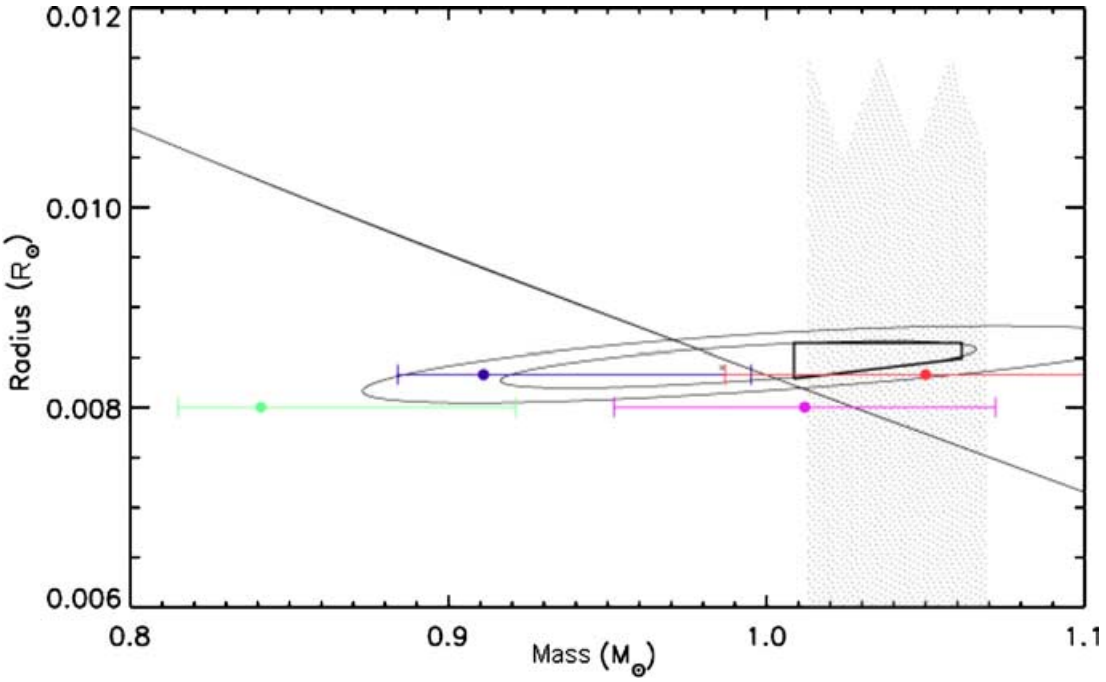

Figure 6. Sirius B mass and radius in solar units compared to the mass–radius relation for carbon-core white dwarfs. The two ellipsoidal contours are the 1σ and 2σ regions determined by Holberg et al. (1998). The vertical stippled region is the range of the astrometric mass determined by Gatewood & Gatewood (1978) while the heavy trapezoid is the joint 1σ spectroscopic and astrometric estimate of Holberg et al. (1998). The sloping black curve is the theoretical mass-radius relation for a ∼25 000 K DA white dwarf with a C–O core (Wood 1995). The upper error bars are those corresponding to the G750M measurement with the mass derived from the surface gravity on the left and that from the gravitational redshift on the right [dark grey (blue on-line) and mid-grey (red) crosses, respectively]. The lower pair of error bars [light grey (green) and mid-grey (purple)] are the corresponding mass determinations for the lower radius obtained from the G430L results.

is illustrated in Fig. 6. A method for combining all the previously available data has been described by Holberg et al. (1998), and we compare that analysis with the new values of M and R listed in Table 5 and shown in Fig. 6. This shows 1σ and 2σ error regions determined by Holberg et al. (1998) together with the allowed astrometric mass range from Gatewood & Gatewood (1978). As we have no information on which of the G430L or G750M flux levels yields the 'best' determination of the white dwarf radius, we plot both sets of results. The upper error bars are those corresponding to the G750M measurement with the mass derived from the surface gravity on the left and that from the gravitational redshift on the right [dark grey (blue on-line) and mid-grey (red) crosses, respectively]. The lower pair of error bars (green and purple) are the corresponding mass determinations for the lower radius obtained from the G430L results.

Although the different determinations of M are not significantly different outside the assigned 1σ uncertainties ranges, it is a concern that we do not obtain better agreement between the various methods of determining M. In theory, it should be possible to treat the data we have obtained with the *HST* in the manner described by Holberg et al. (1998) to determine a 'best-fitting' mass. However, if we do this with our results, the χ^2 minimization technique is rather unstable and very sensitive to the adopted 1σ errors, the values of which are themselves uncertain in the light of the systematic effects we have discussed in this paper. Therefore, we do not believe that the Holberg et al. (1998) method will give a reliable result with the current data.

Comparing the values of M and R obtained in this work with the earlier results is interesting. Individually, only the G430L/surface gravity measurement of M is incompatible with Holberg et al. (1998). However, if the astrometric mass determination is taken into account, only the values of M derived from the gravitational redshift are consistent. Of the measurements we have made, the most problematic is the determination of the stellar radius. Using the narrow slit, it is possible that there could be a loss of light and, as a result, an erroneously low flux determination. This would lead to a low estimate for the white dwarf radius. We have tried to take account of this possibility in the assignment of experimental errors. However, if there really were a light loss at the ∼5 per cent level (the extreme possibility) the overall agreement between the mass determinations would be improved. An independent measurement of the white dwarf flux would be helpful in resolving this question.

Although the main theme of this analysis has been to obtain measurements of M and R that are independent of the white dwarf evolutionary models, given the difficulty in obtaining a reliable stellar radius (on which our measurements depend), it is worthwhile carrying out an empirical determination of M using them. Taking the values of $T_{\rm eff}$ and $\log g$ determined in this paper, we interpolate between the evolutionary models of Wood (1995), which are computed for discrete white dwarf masses in steps of 0.2 $M_\odot$, obtaining $M = 0.978 \pm 0.005$ $M_\odot$ and $R = 0.00864 \pm 0.00012$ $R_\odot$ for Sirius B. The corresponding gravitational redshift is 72.0 ± 1.0 km s^{-1}. We note that, as in the discussion in Section 3.1 on the spectral analysis, the formal errors quoted here are probably factors ∼5–10 too small if we adopt errors for $T_{\rm eff}$ and $\log g$ typical of the ground-based studies. With this in mind, these empirical values of M and R are consistent with those obtained directly from the STIS observations, provided we adopt the flux level taken from the G750M observation rather than the more thoroughly calibrated G430M.

The evolutionary calculations of mass and radius can also be compared to our new measurement of the gravitational redshift, as

this gives a value (126.4 ± 7.6) for M/R directly. Matching this to the relation of Wood (1995) shown in Fig. 6 yields $M = 1.02 \pm 0.02$ and $R = 0.0081 \pm 0.0002$. Importantly, these estimates are not dependent on the model atmosphere calculations, unlike the values derived from the $T_{\rm eff}$ and $\log g$ measurements, and probably have a more robust error determination. Within the overall uncertainties, there is internal consistency between the various methods we have discussed for obtaining M and R. They are also in agreement with the earlier study of Holberg et al. (1998).

5 CONCLUSION

We have obtained an exquisite spectrum of the complete Balmer line series for Sirius B. This is the first such spectrum to be acquired, apart from old ground-based photographic spectra, and can be used to provide an important determination of the stellar temperature ($T_{\rm eff} = 25193 \pm 37$ K) and gravity ($\log g = 8.566 \pm 0.010$). In addition, we have obtained a new, more accurate, gravitational redshift of 80.42 ± 4.83 km s^{-1} for Sirius B. Combining these results with the photometric information available in our spectra and the *Hipparcos* parallax, we have provided new determinations of the stellar mass and radius for comparison with the theoretical mass–radius relation. However, there are some disparities between the values of stellar mass obtained by two different routes, and we have identified significant systematic uncertainties that make the observational errors larger than we had hoped. While we have attempted to make measurements of the mass and radius of the white dwarf independently of the evolutionary model calculations (e.g. Wood 1992, 1995), we obtain much better agreement between our results and those of other authors if we use our spectroscopic measurements of $T_{\rm eff}$ and $\log g$ in conjunction with the theoretical mass–radius relation. Our best estimates of M and R from this approach are 0.978 ± 0.005 M$_\odot$ and 0.00864 ± 0.00012 R$_\odot$, respectively. The gravitational redshift gives us an estimate of M/R directly, which can also be compared to the Wood (1995) models, yielding $M = 1.02 \pm 0.02$ and $R = 0.0081 \pm 0.0002$. These values are all in good agreement with the measurements of other authors and internally consistent with our independent measurements, provided we utilize the stellar absolute flux obtained from the G750M grating.

A particular problem we have encountered is that of possible light loss due to the use of the narrow 50×0.2 arcsec^2 slit, yielding a measured flux for Sirius B lower than the true value. Indeed, the better consistency of results derived from the G750M flux compared to the better calibrated G430L data is indicative of a problem. We anticipate that it will be possible to improve on the measurement derived from our STIS spectra in the future, by making use of the WFPC2 images we have acquired for the study of the binary orbit. In addition, with a wealth of other data also available from soft X-ray, extreme ultraviolet and far-ultraviolet wavebands, an important exercise will be to combine all the information we have to provide the best possible estimate of the mass and radius of Sirius B.

ACKNOWLEDGMENTS

These observations were obtained through the Guest Observer programme of the *HST*. We are grateful to the support astronomers involved for their assistance in scheduling this difficult observation. We would particularly like to thank Charles Proffitt for his assistance in understanding the calibration issues for these spectra and for providing important information that is not yet available in the public domain. MAB and MRB acknowledge the support of the UK Particle Physics and Astronomy Research Council. JBH wishes to acknowledge support from Space Telescope Science Institute grant GO 09762.

REFERENCES

Adams W. S., 1915, PASP, 27, 236
Adams W. S., 1925, Proc. Nat. Acad. Sci. USA, 11, 382 (reprinted in 1925, Observatory, 36, 2)
Aitken R. G., 1918, PASP, 30, 311
Barstow M. A., Good S. A., Burleigh M. R., Hubenz I., Holberg J. B., Levan A. J., 2003a, MNRAS, 344, 562
Barstow M. A. et al., 2003b, MNRAS, 341, 870
Bergeron P., Saffer R. A., Liebert J., 1992, ApJ, 394, 228
Bessel F. W., 1844, MNRAS, 6, 136
Bessell M. S., Castelli F., Plez B., 1998, A&A, 333, 231
Bohlin R. C., 2000, AJ, 120, 437
Bohlin R. C., 1998, STIS Intrument Science Reports (http://www.stsci.edu/hst/stis/documents/isrs), ISR 98-20, 'Clear Aperture Fractional Transmission for Point Sources'
Bohlin R. C., Gilliand R. L., 2004, AJ, 127, 3508
Bohlin R. C., Dickinson M. E., Calzetti D., 2001, AJ, 122, 2118
Campbell W. W., 1905, PASP, 17, 66
Cohen M., Megeath S. T., Hammersley P. L., Fabiola, M.-L., Stauffer J., 2003, ApJ, 125, 2645
Finley D. S., Koester D., Basri G., 1997, ApJ, 488, 375
Gatewood G. D., Gatewood C. V., 1978, ApJ, 225, 191
Grabowski B., Halenka J., Madej J., 1987, ApJ, 313, 750
Greenstein J. L., Oke J. B., Shipman H. L., 1971, ApJ, 169, 563
Greenstein J. L., Oke J. B., Shipman H. L., 1985, QJRAS, 26, 279
Holberg J. B., Wesemael F., Hubeny I., 1984, ApJ, 280, 679
Holberg J. B., Barstow M. A., Bruhweiler F. C., Cruise A. M., Penny A. J., 1998, ApJ, 497, 935
Kidder K., Holberg J. B., Wesemael F., 1989, in Wegner G., ed., White Dwarfs. Lecture Notes in Physics Vol. 328. Springer-Verlag, Berlin, p. 350
Kim Quijano J. et al., 2003, STIS Instrument Handbook, Version 7.0. STSci, Baltimore
Kodaira K., 1967, PASJ, 19, 172
Koester D., 1979, A&A, 72, 376
Landolt A. U., 1992, AJ, 104, 340
Lemke M., 1997, A&AS, 122, 285
Liebert J., Bergeron P., Holberg J. B., 2005, ApJS, 156, 47
Moore J. H., 1928, PASP, 40, 229
Paerels F. B. S., Bleeker J. A. M., Brinkman A. C., Heise J., 1988, ApJ, 329, 849
Rakos K. D., Havlen R. J., 1977, A&A, 61, 185
van den Bos W. H., 1960, Journal des Observateurs, 43, 145
Wesemael F., 1985, QJRAS, 26 273
Wiese W. L., Kelleker D. E., 1971, ApJ, 166, L59
Wood M. A., 1992, ApJ, 386, 539
Wood M. A., 1995, in Koester D., Werner K., eds, Lecture Notes in Physics, White Dwarfs. Springer-Verlag, Berlin, p. 41

This paper has been typeset from a Microsoft Word file prepared by the author.